

# The Preparation and Structure of $[\text{Pt}(\text{S}_2\text{N}_2)\{\text{P}(\text{OR})_n\text{R}'_{3-n}\}_2]$ and $[\text{Pt}(\text{SeSN}_2)\{\text{P}(\text{OMe})_n\text{Ph}_{3-n}\}_2]$ ( $n = 0-3$ )

Paul G. Waddell,<sup>[a]</sup> Alexandra M. Z. Slawin,<sup>[a]</sup> Nicolas Sieffert,<sup>[a]</sup> Michael Bühl,<sup>[a]</sup> and J. Derek Woollins<sup>\*[a]</sup>

**Keywords:** Sulfur / Selenium / Platinum / DFT calculations

Dissolution of  $[\text{S}_4\text{N}_3]\text{Cl}$  in liquid ammonia produces a reactive solution which on treatment with *cis*  $[\text{PtCl}_2(\text{PR}_3)_2]$  gives  $[\text{S}_2\text{N}_2]^{2-}$  complexes in 32–76 % yields. Similarly,  $\text{SeCl}_4$  and  $[\text{S}_4\text{N}_3]\text{Cl}$  in a ratio of 5:1 react cleanly with *cis*- $[\text{PtCl}_2\{\text{P}(\text{OMe})_n\text{Ph}_{3-n}\}]$  to give the desired selenosulfur dinitrido,  $[\text{SeSN}_2]^{2-}$  complexes with no phosphorus containing starting material evident by  $^{31}\text{P}$  NMR spectroscopy. The new complexes were characterised by IR,  $^{31}\text{P}$  NMR, microanalysis and X-ray crys-

tallography with nine crystal structures being reported. In  $^{31}\text{P}$  nmr the  $^1J$  PtP coupling constants are influenced by the oxygen content of their phosphorus ligands. In the mixed chalcogen complexes the Pt–N bond lengths appear to follow a simple trend as a consequence of the electronic properties of the phosphorus ligand and these trends can be interpreted empirically by examination of the LUMO but are not well supported by DFT calculations.

## Introduction

The discovery of the unusual electrical properties of  $(\text{SN})_x$  polymer in 1973 led to sustained interest in this area though M–S–N chemistry has been of interest since the 1950s<sup>[1]</sup> and examples are shown in Figure 1. The disulfur dinitride dianion is not known in simple salts but can be isolated in metal complexes and as fragments in heterocycles.<sup>[2–7]</sup> These complexes may be protonated at the metal-coordinated nitrogen and we have previously commented on the structural consequences of this protonation.<sup>[8,9]</sup> M–S–N complexes may be prepared by a variety of routes, e.g. oxidative addition of  $\text{S}_4\text{N}_4$  or  $\text{S}_4\text{N}_4\text{H}_4$  with  $[\text{Pt}(\text{PPh})_4]$ , reaction of  $\text{Na}[\text{S}_3\text{N}_3]$  with  $[\text{PtCl}_2(\text{PR}_3)_2]$  or transmetallation

using  $[\text{Me}_2\text{SnS}_2\text{N}_2]_2$  or  $[\text{nBu}_2\text{SnS}_2\text{N}_2]_2$ . We have also shown the value of the use of  $[\text{S}_4\text{N}_3]\text{Cl}$  in liquid ammonia as a solvent in these reaction systems but have not established it for the synthesis of  $\text{M}(\text{S}_2\text{N}_2)$  systems.<sup>[10,11]</sup>

Surprisingly there is some ambiguity about the bond length pattern in some  $[\text{Pt}(\text{S}_2\text{N}_2)(\text{PR}_3)_2]$  complexes<sup>[14]</sup> and there is only one example of a  $[\text{Pt}(\text{S}_2\text{N}_2)\{\text{P}(\text{OR})_3\}_2]$  complex whose formulation was proposed using only IR spectroscopy and microanalysis data.<sup>[15]</sup> The formulation of this complex remains doubtful.

In addition to  $[\text{S}_2\text{N}_2]^{2-}$  complexes, some selenium-substituted analogues have been investigated.<sup>[16–21]</sup> As yet only one  $[\text{SeSN}_2]^{2-}$  containing complex  $[\text{Pt}(\text{SeSN}_2)(\text{PMe}_2\text{Ph})_2]$  has been analysed using X-ray crystallography and this ex-

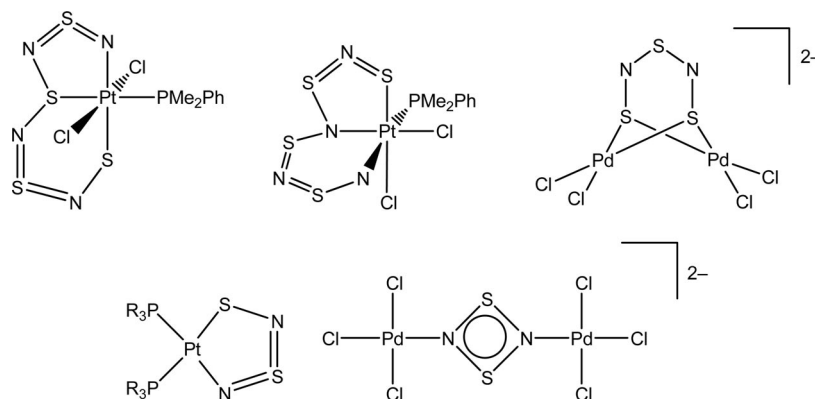


Figure 1. Examples of fully characterised M–S–N species.<sup>[12,13]</sup>

[a] School of Chemistry, University of St Andrews, St Andrews, Scotland, KY16 9ST  
E-mail: jdw3@st-and.ac.uk

ample was found to exhibit a twofold disorder about the ring. Given the need to develop routes in liquid ammonia, the lack of crystal data for selenium-substituted analogues

of these complexes, bond length ambiguity mentioned above and the poor understanding of the bonding in these types of molecules we have studied the synthesis, structure and spectroscopic properties of simple  $[\text{Pt}(\text{S}_2\text{N}_2)\{\text{P}(\text{OR})_n\text{R}'_{3-n}\}_2]$  and  $[\text{Pt}(\text{SeSN}_2)\{\text{P}(\text{OMe})_n\text{Ph}_{3-n}\}_2]$  complexes. Here we report the synthesis of several of these  $[\text{Pt}(\text{S}_2\text{N}_2)\{\text{P}(\text{OR})_n\text{R}'_{3-n}\}_2]$  and  $[\text{Pt}(\text{SeSN}_2)\{\text{P}(\text{OMe})_n\text{Ph}_{3-n}\}_2]$  complexes which have been characterised by IR spectroscopy,  $^{31}\text{P}$  NMR spectroscopy, elemental analysis and X-ray crystallography.

## Results and Discussion

There are a number of possible routes to  $[\text{Pt}(\text{S}_2\text{N}_2)\{\text{P}(\text{OR})_3\}_2]$  complexes. Use of  $\text{S}_4\text{N}_4$  or  $[\text{S}_3\text{N}_3]^-$  salts are best avoided because of explosion hazard. We chose to generate the appropriate anion in situ using  $[\text{S}_4\text{N}_3]^- \text{Cl}$  in liquid ammonia which reacted cleanly with *cis*- $[\text{PtCl}_2(\text{PR}_3)_2]$  to give the desired disulfur dinitrido complexes with no phosphorus containing starting material evident by  $^{31}\text{P}$  NMR spectroscopy. Though the mechanism and its stoichiometry are complex and are not completely understood to date, the stoichiometry of 14 equiv. of  $[\text{S}_4\text{N}_3]^- \text{Cl}$  to 9 equiv. of *cis*- $[\text{PtCl}_2(\text{PR}_3)_2]$  is in accord with previously suggested equilibria; see Equations (1)–(3).<sup>[23,24]</sup>



The new complexes **1**,  $\text{PR}_3 = \text{P}(\text{OEt})_3$ ; **2**,  $\text{PR}_3 = \text{P}(\text{O}n\text{Bu})_3$ ; **3**,  $\text{PR}_3 = \text{P}(\text{OPh})_3$ ; **4**,  $\text{PR}_3 = \text{P}(\text{OMe})_3$ ; **5**,  $\text{PR}_3 = \text{P}(\text{OMe})_2\text{Ph}$ ; **6**,  $\text{PR}_3 = \text{P}(\text{OMe})_2\text{Ph}$  were characterised by  $^{31}\text{P}$  NMR (Table 1), IR, microanalysis (Table 2) and X-ray crystallography. In their IR spectra the important  $\nu_{\text{SN}}$  vibrations were assigned by analogy with previously reported  $[\text{Pt}(\text{S}_2\text{N}_2)(\text{PR}_3)_2]$  complexes.<sup>[2]</sup> However, the presence of the  $\nu_{(\text{P}-\text{O}-\text{alkyl})}$  vibration ( $1050\text{--}1030\text{ cm}^{-1}$ ) obscures one of the  $\nu_{\text{SN}}$  vibrations, which is normally observed around  $1050\text{ cm}^{-1}$  for **1** and **4** though the band at around  $680\text{ cm}^{-1}$  is not obscured. The intensity of the  $\nu_{(\text{P}-\text{O}-\text{alkyl})}$  vibration ( $1050\text{--}1030\text{ cm}^{-1}$ ) increases with the oxygen content as would be expected. Distinct vibrations due to the P-Ph group (approx.  $1440\text{ cm}^{-1}$ ) were also observed for **5** and **6**.

Mixed-chalcogen compounds containing the  $[\text{SeSN}_2]^{2-}$  fragment have been synthesised using  $[\text{Se}_2\text{SN}_2]_2\text{Cl}_2$  or a combination of  $\text{SeCl}_4$  and  $[\text{S}_4\text{N}_3]^- \text{Cl}$  in liquid ammonia. The nature of the species in the liquid ammonia solution has not been determined. As dissolution of  $[\text{S}_4\text{N}_3]^- \text{Cl}$  in liquid ammonia results in formation of  $[\text{S}_3\text{N}_3]^-$  it is possible that this species is in equilibrium with a range of change SN anions which can undergo chalcogen exchange to give mixed SeSN anions. The formation of the  $\text{PtSeSN}_2$  rings with selenium always platinum-bound may suggest that the SeSN anions have terminal selenium atoms. Certainly we would expect that SeNSN would be a more stable isomer than SNSN. Furthermore SeNSN could be readily formed by chain lengthening of the well know  $[\text{NSN}]^{2-}$  dianion.<sup>[25]</sup> After a number of trials we employed  $\text{SeCl}_4$  and  $[\text{S}_4\text{N}_3]^- \text{Cl}$  in a ratio of 5:1 which reacted cleanly with *cis*- $[\text{PtCl}_2(\text{P}(\text{OMe})_n\text{Ph}_{3-n})]$  to give the desired selenosulfur dinitrido complexes with no phosphorus containing starting material evident by  $^{31}\text{P}$  NMR spectroscopy however trace amounts of the disulfur analogue were observed.

The new complexes  $[\text{Pt}(\text{SeSN}_2)\{\text{P}(\text{OMe})_n\text{Ph}_{3-n}\}_2]$  (**7**,  $n = 3$ , **8**,  $n = 2$ , **9**,  $n = 1$ ) were characterised by  $^{31}\text{P}$  NMR, IR, microanalysis (Table 1, 2) and X-ray crystallography. The X-ray of the previously reported complex **10** ( $n = 0$ ) was also determined. In their IR spectra the vibrations due characteristic of the  $[\text{SeSN}_2]^{2-}$  fragment were assigned by analogy with previously reported  $[\text{Pt}(\text{SeSN}_2)(\text{PR}_3)_2]$  complexes.<sup>[21]</sup> In the case of **9** the  $\nu_{\text{SN}}$  vibration typically observed at ca.  $1070\text{ cm}^{-1}$  was slightly lower than expected ( $1059\text{ cm}^{-1}$ ). The corresponding stretch observed in  $[\text{S}_2\text{N}_2]^{2-}$  complexes is observed at ca.  $1045\text{ cm}^{-1}$ . Vibrations indicative of  $\nu_{\text{PtSe}}$  were not observed and are likely to be very low in frequency compared to the  $\nu_{\text{PtS}}$  stretch in  $[\text{S}_2\text{N}_2]^{2-}$  complexes (ca.  $350\text{ cm}^{-1}$ ) due to the larger mass of selenium compared to sulfur. The intensity of the  $\nu_{(\text{P}-\text{O}-\text{alkyl})}$  vibration ( $1050\text{--}1030\text{ cm}^{-1}$ ) increases with the oxygen content as would be expected. Distinct vibrations due to the P-Ph group (approx.  $1440\text{ cm}^{-1}$ ) were also observed for **8** and **9**.

The  $^{31}\text{P}$  NMR of **1–10** exhibit AX doublets (Table 1, see Figure 2 for labelling and Figure 3 for a typical spectrum) with  $^2J_{\text{P,P}}$  couplings together with satellites due to  $^1J_{\text{Pt,P}}$  couplings. **7–10** also exhibit  $^2J_{\text{P-Se(trans)}}$  couplings<sup>[26]</sup> though  $^2J_{\text{P-Se(cis)}}$  couplings were not observed. These couplings en-

Table 1.  $^{31}\text{P}$  NMR chemical shifts (ppm) and coupling constants (Hz) for **1–10** and  $[\text{Pt}(\text{S}_2\text{N}_2)(\text{PPh}_3)_2]$ .

	$\delta_{\text{A}}$	$\delta_{\text{X}}$	$^1J_{\text{A}}$	$^1J_{\text{X}}$	$^2J_{\text{P-P}}$	$^2J_{\text{P-Se(trans)}}$
$[\text{Pt}(\text{S}_2\text{N}_2)\{\text{P}(\text{OEt})_3\}_2]$ ( <b>1</b> )	98.5	105.5	4498	4415	49.3	
$[\text{Pt}(\text{S}_2\text{N}_2)\{\text{P}(\text{O}n\text{Bu})_3\}_2]$ ( <b>2</b> )	102.8	109.0	4470	4334	49.3	
$[\text{Pt}(\text{S}_2\text{N}_2)\{\text{P}(\text{OPh})_3\}_2]$ ( <b>3</b> )	89.6	96.7	4634	4503	54.0	
$[\text{Pt}(\text{S}_2\text{N}_2)\{\text{P}(\text{OMe})_3\}_2]$ ( <b>4</b> )	105.3	110.9	4502	4395	51.0	
$[\text{Pt}(\text{S}_2\text{N}_2)\{\text{P}(\text{OMe})_2\text{Ph}\}_2]$ ( <b>5</b> )	120.4	126.2	3864	3761	37.6	
$[\text{Pt}(\text{S}_2\text{N}_2)\{\text{P}(\text{OMe})\text{Ph}_2\}_2]$ ( <b>6</b> )	91.8	104.1	3287	3249	28.2	
$[\text{Pt}(\text{S}_2\text{N}_2)(\text{PPh}_3)_2]$	11.4	23.6	2994	2827	22	
$[\text{Pt}(\text{SeSN}_2)\{\text{P}(\text{OMe})_3\}_2]$ ( <b>7</b> )	106.0	108.1	4530	4571	49	94
$[\text{Pt}(\text{SeSN}_2)\{\text{P}(\text{OMe})_2\text{Ph}\}_2]$ ( <b>8</b> )	122.9	124.8	3868	3900	33	75
$[\text{Pt}(\text{SeSN}_2)\{\text{P}(\text{OMe})\text{Ph}_2\}_2]$ ( <b>9</b> )	89.3	103.1	3309	3391	26	66
$[\text{Pt}(\text{SeSN}_2)\{\text{P}(\text{Ph})_3\}_2]$ ( <b>10</b> )	7.2	22.6	2995	2956	21	54

Table 2. Microanalyses, yields, melting points and selected IR absorptions with tentative assignments [cm<sup>-1</sup>] for **1** and **3–9**.<sup>[a]</sup>

	$\tilde{\nu}_{\text{SN}}$	$\nu_{\text{SN/SeN}}$	$\nu_{\text{PtN}}$	$\delta_{\text{SN}}$	$\nu_{\text{PtS}}$	% C (calcd.)	% H (calcd.)	Yield (%)	M.p. (°C)
[Pt(S <sub>2</sub> N <sub>2</sub> ){P(OEt) <sub>3</sub> ] <sub>2</sub> ] ( <b>1</b> )	686 s <sup>[b]</sup>	618 m	469 m	370 m	354 m	23.25 (23.26)	4.78 (4.88)	47	138–142
[Pt(S <sub>2</sub> N <sub>2</sub> ){P(OPh) <sub>3</sub> ] <sub>2</sub> ·0.5CH <sub>2</sub> Cl <sub>2</sub> ( <b>3</b> )	687 s <sup>[b]</sup>	618 m	491 s	380 w	357 w	45.90 (46.13)	3.12 (3.28)	32	117–120
[Pt(S <sub>2</sub> N <sub>2</sub> ){P(OMe) <sub>3</sub> ] <sub>2</sub> ] ( <b>4</b> )	682 s <sup>[b]</sup>	614 w	467 w	372 m	354 w	13.23 (13.46)	3.08 (3.39)	58	123–125
	1094(17) 727(10)	648(3) <sup>[c]</sup>	492(2) <sup>[d]</sup>	366(2) <sup>[e]</sup>	362(1)				
[Pt(S <sub>2</sub> N <sub>2</sub> ){P(OMe) <sub>2</sub> Ph] <sub>2</sub> ·0.5CH <sub>2</sub> Cl <sub>2</sub> ( <b>5</b> )	1047 s 684 m	613 m	467 m	371 m	355 m	29.74 (29.58)	3.38 (3.46)	62	139–142
[Pt(S <sub>2</sub> N <sub>2</sub> ){P(OMe)Ph <sub>2</sub> ] <sub>2</sub> ] ( <b>6</b> )	1042 s 680 m	615 w	462 m	360 w	349 w	43.22 (43.39)	3.79 (3.64)	60	160–163
[Pt(SeSN <sub>2</sub> ){P(OMe) <sub>3</sub> ] <sub>2</sub> ] ( <b>7</b> )	1068s 633m	541 m	401 w	357 w		12.76 (12.37)	2.70 (3.12)	76	132–134
	1110(10) 659(7) <sup>[f]</sup>	580(3) <sup>[g]</sup>	428(1) <sup>[d]</sup>	360(2) <sup>[e]</sup>	246(1) <sup>[g]</sup>				
[Pt(SeSN <sub>2</sub> ){P(OMe) <sub>2</sub> Ph] <sub>2</sub> ·0.5CH <sub>2</sub> Cl <sub>2</sub> ( <b>8</b> )	1071 s 634 m	556 s	402 m	357 m		27.38 (27.64)	2.82 (3.23)	51	184–187
[Pt(SeSN <sub>2</sub> ){P(OMe)Ph <sub>2</sub> ] <sub>2</sub> ·0.5CH <sub>2</sub> Cl <sub>2</sub> ( <b>9</b> )	1059 s 634 m	542 s	402 w	355 w		39.42 (39.34)	2.96 (3.36)	63	146–149

[a] Printed in *italics*: PBE0/ECPI computed harmonic frequencies (in parentheses: intensities in 104 M/mol; maximum absorption around 60.104 M/mol). [b] Band obscured by P–O–alkyl absorption. [c] Combination with  $\delta_{\text{NSN}}$  and  $\delta_{\text{PtNS}}$ . [d] Combination with  $\delta_{\text{SNS}}$ . [e] SN2 out-of-plane. [f] Combination of  $\nu_{\text{sym,PtN/SeN}}$  and  $\delta_{\text{NSN}}$ . [g]  $\nu_{\text{asym,PtN/SeN}}$ . *lv*, PtSe.

abled assignment of the individual phosphorus resonances. By analogy with phosphane complexes, the largest  $^1J(^{195}\text{Pt}-^{31}\text{P})$  coupling constant in [S<sub>2</sub>N<sub>2</sub>]<sup>2-</sup> complexes is assigned to the phosphorus *trans* to the nitrogen ( $\delta_{\text{A}}$ ) as this platinum–phosphorus bond is generally the shorter of the two and the shorter distance can be associated with the larger coupling constant. The smaller of the two  $^1J_{\text{Pt,P}}$  values is assigned to the phosphorus *trans* to sulfur ( $\delta_{\text{X}}$ ). In [SeSN<sub>2</sub>]<sup>2-</sup> complexes similar  $^1J_{\text{A}}$  values are observed to those in [S<sub>2</sub>N<sub>2</sub>]<sup>2-</sup> complexes however in the case the  $^1J_{\text{X}}$  (the phosphorus *trans* to selenium is the larger value).

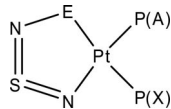


Figure 2. Labelling of the phosphorus atoms (E = S or Se).

As expected the coupling constants for **1** to **10** are influenced by the phosphorus ligands. The effect of replacing phenyl groups of the phosphanes with methyl groups in [S<sub>2</sub>N<sub>2</sub>]<sup>2-</sup> complexes has been previously reported,<sup>[2]</sup> with  $^1J_{\text{Pt-P}}$  being observed to decrease in the order PPh<sub>3</sub> > PMePh<sub>2</sub> > PMe<sub>2</sub>Ph > PMe<sub>3</sub>. The effect of replacing phenyl groups in the phosphorus ligand with methoxy groups has the opposite effect in both [S<sub>2</sub>N<sub>2</sub>]<sup>2-</sup> and [SeSN<sub>2</sub>]<sup>2-</sup> complexes with the coupling constants increasing in the order PPh<sub>3</sub> < P(OMe)Ph<sub>2</sub> < P(OMe)<sub>2</sub>Ph < P(OMe)<sub>3</sub> (Table 1, Figures 4 and 5).

Comparing  $^1J_{\text{Pt,P}}$  values observed for [S<sub>2</sub>N<sub>2</sub>]<sup>2-</sup> and [SeSN<sub>2</sub>]<sup>2-</sup> complexes with the same phosphorus ligand with those of their dichloride starting materials gives some indi-

cation as to the *trans*-influence<sup>[27,28]</sup> of the chalcogen–nitrogen fragments. From the coupling constants we can see that the *trans* influence of the [S<sub>2</sub>N<sub>2</sub>]<sup>2-</sup> fragment is greater than that of the chlorine atoms as the coupling constants are seen to decrease by over 20% for both P<sub>A</sub> and P<sub>X</sub> indicating weaker Pt–P bonds in both cases. When compared with [SeSN<sub>2</sub>]<sup>2-</sup> complexes, the  $^1J_{\text{A}}$  values are observed to be of a similar magnitude and  $^1J_{\text{A}}$  is seen to be ca. 100–200 Hz greater than that observed in [S<sub>2</sub>N<sub>2</sub>]<sup>2-</sup> complexes. The *trans* influence of selenium in the [SeSN<sub>2</sub>]<sup>2-</sup> fragment can hence be said to be less than that of the sulfur in the [S<sub>2</sub>N<sub>2</sub>]<sup>2-</sup> fragment.

The co-ordination shifts of the [Pt(S<sub>2</sub>N<sub>2</sub>)(PR<sub>3</sub>)<sub>2</sub>] (R = alkyl, aryl) relative to their [PtCl<sub>2</sub>(PR<sub>3</sub>)<sub>2</sub>] starting materials are about –8 ppm for  $\delta_{\text{A}}$  and about +7 ppm for  $\delta_{\text{X}}$ . For the phosphite-containing complexes the chemical shifts also exhibit a relatively constant co-ordination shift compared to their starting materials:  $\delta_{\text{A}}$  is shifted by ca. +31 ppm and  $\delta_{\text{X}}$  by ca. +37 ppm for all the phosphite systems. The chemical shifts for **7–10** were found to be similar to their [S<sub>2</sub>N<sub>2</sub>]<sup>2-</sup> analogues.

The  $^2J_{\text{P,P}}$  coupling constants increase in the order PPh<sub>3</sub> < P(OMe)Ph<sub>2</sub> < P(OMe)<sub>2</sub>Ph < P(OMe)<sub>3</sub> from ca. 22 Hz to ca. 49 Hz presumably reflecting the relative Pt–P bond strengths in this series. Similarly  $^2J_{\text{P-Se(trans)}}$  for **7–10** decreases from 94 to 60 Hz. No *cis*-selenium satellites were observed and given the small magnitudes of previously reported  $^2J_{\text{P-Se(cis)}}$  values this is understandable.<sup>[26]</sup>

The structures of the [S<sub>2</sub>N<sub>2</sub>]<sup>2-</sup> complexes **1** and **3–6** (Table 3, Figures 6 and 7) exhibit square-planar geometry about platinum. The Pt–P distances (Table 3, Figure 8) lie in the range 2.217(3) Å and 2.256(2) Å. One might antici-

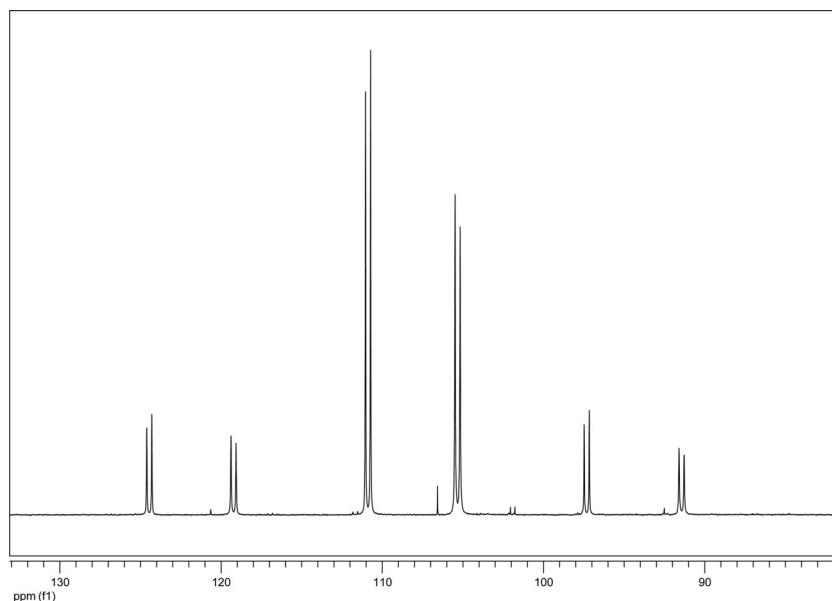


Figure 3.  $^{31}\text{P}\{^1\text{H}\}$  NMR spectrum (109 MHz,  $\text{CH}_2\text{Cl}_2$  solution) of **4**.

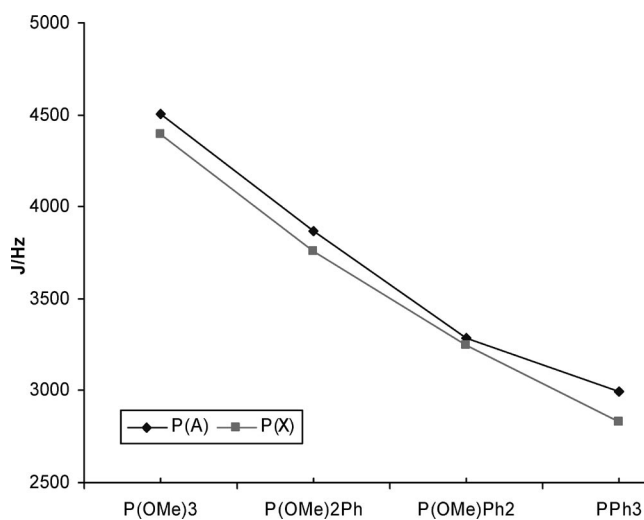


Figure 4. Variation of  $^1J_A$  and  $^1J_X$  in  $[\text{Pt}(\text{S}_2\text{N}_2)\{\text{P}(\text{OMe})_n\text{Ph}_{3-n}\}]_2$  complexes.

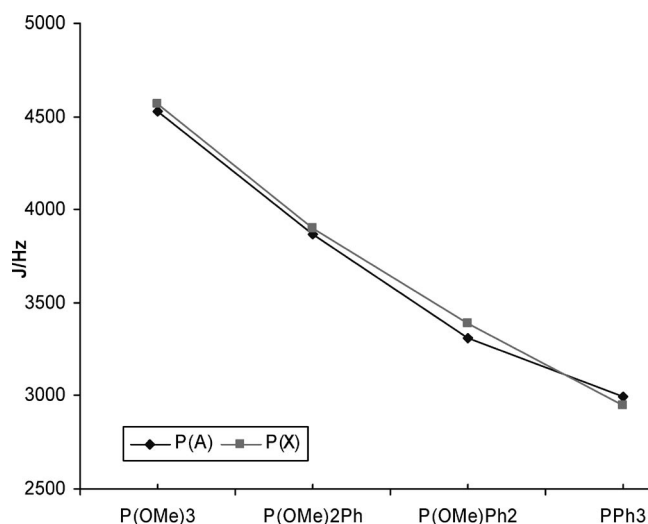


Figure 5. Variation of  $^1J_A$  and  $^1J_X$  in  $[\text{Pt}(\text{SeSN}_2)\{\text{P}(\text{OMe})_n\text{Ph}_{3-n}\}]_2$  complexes.

pate a difference in Pt–P bond length *trans* to sulfur versus *trans* to nitrogen and there does appear to be a trend suggesting that Pt–P(2) (*trans* to nitrogen) is usually shorter [i.e. for those where there is a structurally relevant difference, Pt–P(2) is shorter than Pt–P(1)]. In general all of the Pt–P distances observed for **1** and **3–6** are longer than for the chloride complexes. The Pt–N bond lengths are in the range 2.016(4)–2.070(7) Å and the Pt–S bond lengths are in the range 2.289(2)–2.295(3) Å. The Pt–N distance appears more sensitive to the nature of the phosphane/phosphite though we cannot see any direct trends.

As changing the phosphorus ligands gave rise to trends in coupling constants in  $^{31}\text{P}$  NMR we wondered if we might see an effect on the geometry of the metal sulfur–nitrogen ring complexes. On the whole however this effect was not

measurable crystallographically. The bond lengths and angles are comparable to equivalent complexes with phosphane ligands with two short sulfur–nitrogen bonds, which are slightly longer than a typical sulfur–nitrogen double bond (1.45 Å) ranging from 1.515(8)–1.590(9) Å and one long sulfur–nitrogen bond, which corresponds to the length of a typical sulfur–nitrogen single bond (1.69 Å) ranging from 1.673(9)–1.709(11) Å. There is a small departure from this trend in the case of **6** for which there is one short, one long and one medium intermediate length bond indicating some degree of electron delocalisation. If the S–N bond lengths in **1** are discounted (since this structure contains significant disorder) then the average bond lengths for the remaining structures are N(1)–S(1) 1.54(2), S(1)–N(2) 1.58(2) and S(2)–N(2) 1.69(2) Å. Bond angles within the

Table 3. Selected bond lengths [Å] and angles [°] for **1**, **3–6** and [Pt(S<sub>2</sub>N<sub>2</sub>)(PPh<sub>3</sub>)<sub>2</sub>]. Values printed in *italics* are DFT-calculated parameters (asterisks \* denote two-fold disorder).

	<b>1</b>	<b>3</b>	<b>4</b>	<b>5</b>	<b>6</b>	[Pt(S <sub>2</sub> N <sub>2</sub> )(PPh <sub>3</sub> ) <sub>2</sub> ]-4CH <sub>2</sub> Cl <sub>2</sub> <sup>[7]</sup>	[Pt(S <sub>2</sub> N <sub>2</sub> )(PPh <sub>3</sub> ) <sub>2</sub> ]-C <sub>7</sub> H <sub>8</sub> <sup>[4]</sup>
Pt–N(1)	2.050(17)	2.057(11)	2.064(8)	2.016(4)	2.070(7)	2.018(4)	2.093(13)
Pt–S(2)	2.293(9)	2.291(3)	2.295(3)	2.2923(15)	2.289(2)	2.288(5)	2.294(6)
Pt–P(1)	2.237(2)	2.234(3)	2.246(3)	2.2407(15)	2.256(2)	2.317(4)	2.308(5)
Pt–P(2)	2.239(2)	2.221(3)	2.217(3)	2.2175(15)	2.250(2)	2.263(4)	2.259(3)
N(1)–S(1)	1.69(2)*	1.541(11)	1.544(13)	1.572(5)	1.515(8)	1.546(16)	1.499(16)
S(1)–N(2)	1.46(2)*	1.589(13)	1.554(13)	1.568(5)	1.590(9)	1.567(19)	1.702(15)
N(2)–S(2)	1.763(17)*	1.689(12)	1.709(11)	1.702(5)	1.673(9)	1.682(16)	1.548(12)
P(1)–Pt–P(2)	93.57(7)	96.18(11)	93.89(15)	95.12(6)	96.14(7)	98.4(1)	97.8(1)
N(1)–Pt–S(2)	90.5(5)	88.5(3)	87.8(4)	88.78(15)	87.0(2)	87.6(5)	86.8(4)
Pt–N(1)–S(1)	109.5(10)	114.6(6)	115.0(7)	115.1(3)	115.6(4)	116.2(9)	113.5(7)
N(1)–S(1)–N(2)	120.6(12)	116.9(6)	117.2(6)	116.7(3)	117.0(4)	116.0(9)	117.5(7)
S(1)–N(2)–S(2)	115.2(14)	116.3(6)	116.6(7)	115.8(3)	115.6(5)	116.1(11)	113.7(8)
N(2)–S(2)–Pt	103.3(9)	103.6(4)	103.4(4)	103.60(18)	104.9(3)	104.0(7)	108.4(7)

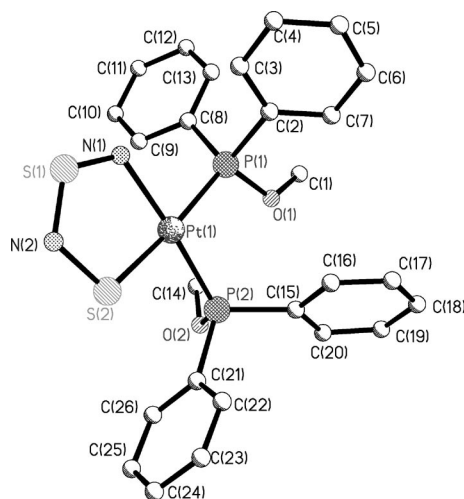


Figure 6. X-ray crystal structure of **6**. The structures of **3–5** are not illustrated as they are similar.

ring were fairly consistent throughout and were comparable to previously reported examples. When compared to the starting materials the bond angle P(1)–Pt–P(2) was observed to be smaller with a range of 96.18(11)–93.57(7) Å.

The structures of the [SeSN<sub>2</sub>]<sup>2-</sup> complexes **7–10** (Table 4, Figure 9) also exhibit square-planar geometry about platinum. Unlike the previously reported structure, none of the structures exhibit detectable disorder. Only **9** was observed to be isomorphous (ie similar unit cell and crystal system) to its [S<sub>2</sub>N<sub>2</sub>]<sup>2-</sup> analogue. Of the bonds within the ring those involving N(1) are most sensitive to the nature of the phosphorus ligand. The Pt–N(1) bond lengths increases from 2.041(9)–2.095(4) Å as the OMe groups are successively replaced by Ph groups ie the phosphane complex has the longest Pt–N(1) bond length. Concurrently, the N(1)–S(1)

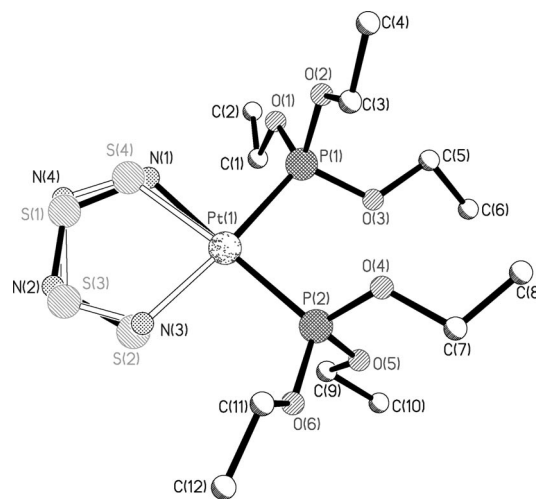


Figure 7. X-ray crystal structure of **1** showing twofold disorder about the [S<sub>2</sub>N<sub>2</sub>]<sup>2-</sup> fragment.

bond length decreases from 1.532(9)–1.480(7) Å with the PPh<sub>3</sub> complex having the shortest N(1)–S(1) distance. Interestingly, and perhaps counter-intuitively, the Pt–P distances in **7–10** [in the range 2.214(2) Å and 2.3069(17) Å] also increase as OMe is replaced by Ph for both Pt–P(1) and Pt–P(2) (Figure 10).

In order to understand these apparent trends in bond lengths we performed DFT calculations on a range of complexes. For compounds **4** and **7**, the DFT-computed IR data are included in Table 2 for comparison. The computed harmonic frequencies are systematically larger than the observed fundamentals (by typically 30–40 cm<sup>-1</sup>), but overall the observed patterns assigned to the metallacycle are reasonably well reproduced computationally. Since the [S<sub>2</sub>N<sub>2</sub>]<sup>2-</sup> ligand often appears to be disordered we included

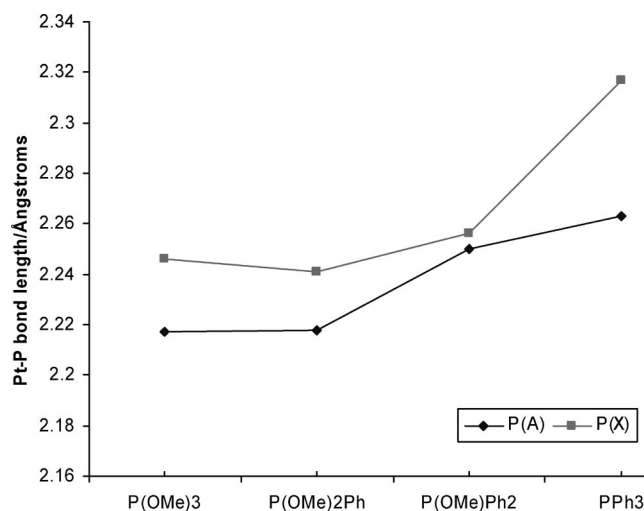


Figure 8. Variation of Pt–P(A) and Pt–P(X) bond lengths in  $[\text{Pt}(\text{S}_2\text{N}_2)\{\text{P}(\text{OMe})_n\text{Ph}_{3-n}\}_2]$  complexes.

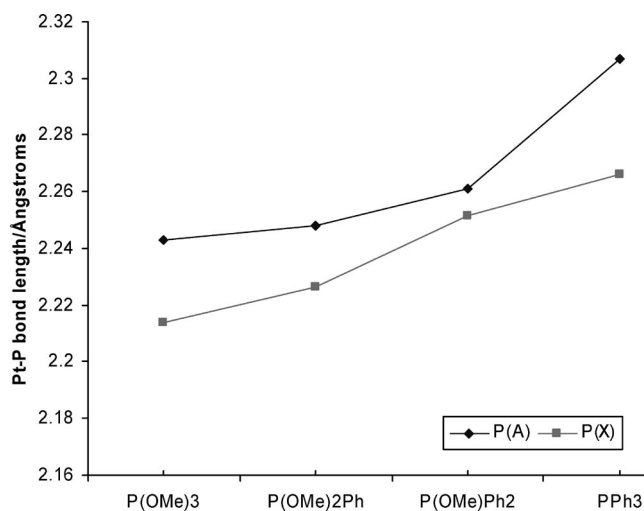


Figure 10. Variation of Pt–P(A) and Pt–P(X) bond lengths in  $[\text{Pt}(\text{SeSN}_2)\{\text{P}(\text{OMe})_n\text{Ph}_{3-n}\}_2]$  complexes.

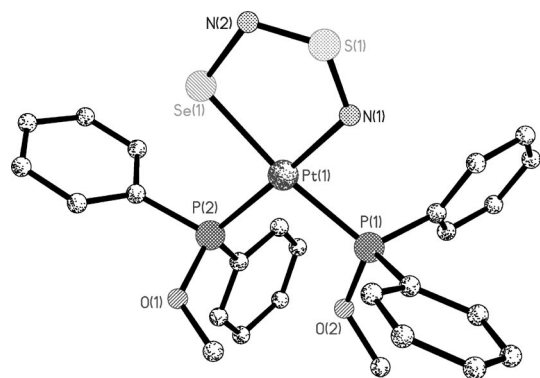


Figure 9. X-ray crystal structure of **9**. The structures of **7**, **8** and **10** are not illustrated as they are similar.

an example of the protonated system which appears more well-behaved crystallographically. The results of the DFT calculations are shown in Tables 3 and 4. It is striking that these calculations, whilst fitting the protonated structures well, do not mirror the observed trends in Pt–N and S–N bond lengths. The DFT calculations suggest that the Pt–N bond length is not significantly influenced by the nature of the *trans* ligand in the compounds studied here. Quite unusually, the DFT-optimised Pt–N distances are noticeably shorter than most of the X-ray data. For the model system  $[\text{Pt}(\text{S}_2\text{N}_2)(\text{PH}_3)_2]$ , PBE0-optimised distances agree well with those obtained at the CCST(T) level, the “gold standard” of ab initio quantum chemistry. There is thus no evidence for a particular DFT problem with this kind of bond.<sup>[29]</sup>

Table 4. Selected bond lengths [Å] and angles [°] for **7–10**. Values printed in *italics* are DFT-calculated parameters.

	<b>7</b>	<b>8</b>	<b>9</b>	<b>10</b>
Pt–N(1)	2.041(9)	2.065(4)	2.074(13)	2.095(4)
	<i>2.025</i>			<i>2.022</i>
Pt–Se(1)	2.3874(11)	2.4099(5)	2.3987(16)	2.3818(9)
	<i>2.423</i>			<i>2.421</i>
Pt–P(1)	2.214(2)	2.2266(13)	2.2517(18)	2.2664(12)
	<i>2.240</i>			<i>2.295</i>
Pt–P(2)	2.243(2)	2.2480(14)	2.2609(16)	2.3069(17)
	<i>2.263</i>			<i>2.338</i>
N(1)–S(1)	1.532(9)	1.523(4)	1.496(15)	1.480(7)
	<i>1.562</i>			<i>1.557</i>
S(1)–N(2)	1.571(7)	1.564(5)	1.547(16)	1.572(6)
	<i>1.564</i>			<i>1.565</i>
N(2)–Se(1)	1.826(9)	1.858(4)	1.858(15)	1.819(5)
	<i>1.838</i>			<i>1.843</i>
P(1)–Pt–P(2)	94.83(9)	94.94(5)	96.29(14)	97.84(5)
	<i>96.9</i>			<i>100.5</i>
P(2)–Pt–Se(1)	174.37(3)	173.45(7)	172.49(4)	170.74(3)
P(1)–Pt–N(1)	179.4(2)	173.80(11)	175.32(16)	176.85(18)
N(1)–Pt–Se(1)	88.0(2)	87.87(12)	86.7(3)	86.31(18)
Pt–N(1)–S(1)	117.9(4)	117.8(2)	119.1(7)	118.5(2)
N(1)–S(1)–N(2)	118.4(4)	119.5(2)	118.8(7)	118.9(2)
S(1)–N(2)–Se(1)	115.0(5)	114.8(2)	115.1(8)	114.8(4)
N(2)–Se(1)–Pt	100.7(2)	100.01(15)	100.2(4)	101.5(2)

We considered that even a small component of disorder in eg the  $[\text{SeSN}_2]^{2-}$  could cause apparent lengthening of the Pt–N bond length and re-examined our crystal structures carefully for residual electron density peaks as well as looking carefully at the thermal parameters. We do not see any evidence of disorder.

The HOMO and LUMO of the  $\text{Pt}(\text{SSeN}_2)$  fragment were examined (Figures 11 and 12). On going from phosphane to phosphite ligands, the weaker  $\sigma$ -donor capability should result in shorter Pt–N and longer N(1)–S(1) bonds (as less electron density is donated into this LUMO). On the other hand, the HOMO has antibonding character for both bonds. The stronger  $\pi$ -acceptor capability of phosphites over phosphanes should thus produce shorter bonds (as more electron density is removed from the HOMO).<sup>[30]</sup> While no clear trend can be predicted for the N(1)–S(1) distance on these grounds, the Pt–N bond should contract with an increasing number of phosphites, in good apparent agreement with the observed trend. So overall we can see that the trends in bond lengths are not well supported by the DFT calculations though empirical arguments based on the LUMO may be used to rationalise the trends. We cannot judge if the difficulties here are a consequence of experimental or computational difficulties.

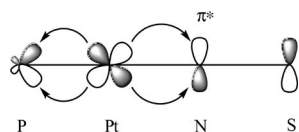


Figure 11. Backbonding from Pt to the  $\pi^*$  orbital on N in the metallacycles studied here.

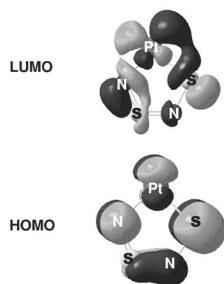


Figure 12. Frontier molecular orbitals of the  $\text{Pt}(\text{S}_2\text{N}_2)$  fragment (in the geometry of the  $\text{PMe}_3$  complex, PBE0/ECP1 level).

The variation in Pt–P bond length can be correlated with the decreasing magnitude of  $^1J_{\text{Pt,P}}$  which is itself a crude measure of bond strength. The remaining three bonds in the metallacycle appear less sensitive to the phosphorus ligand and do not exhibit any distinguishable trend [S(1)–N(2) range 1.547(16)–1.572(6) Å and N(2)–Se(1) range 1.819(5)–1.858(15) Å]. The Pt–Se bond lengths are in the range 2.3818(9)–2.4099(5) Å.

When compared to the  $[\text{S}_2\text{N}_2]^{2-}$  analogues the P(1)–Pt–P(2) bond angles in the mixed-chalcogen complexes are observed to be similar and influenced by the steric bulk of the

phosphorus ligand with a range of 94.83(9)° to 97.84(5)° increasing in the order  $7 < 8 < 9 < 10$ . Similarly the N(1)–Pt–Se angles [which are comparable to the N(1)–Pt–S(2) angles of  $[\text{Pt}(\text{S}_2\text{N}_2)\{\text{P}(\text{OMe})_n\text{Ph}_{3-n}\}_2]$  complexes with a range of 86.31(18)° to 88.0(2)°] increase as the P(1)–Pt–P(2) bond angle decreases, again reflecting the increasing steric bulk of the phosphorus ligands. At the PBE0 level, P–Pt–P bond angles tend to be overestimated by up to ca. 2°, which for  $[\text{Pt}(\text{S}_2\text{N}_2)(\text{PPh}_3)_2]$  is remedied at the dispersion-corrected B97-D level, where a P–Pt–P angle of 97.5° is obtained, in excellent agreement with experiment.

## Conclusions

We have synthesised the series of complexes  $[\text{Pt}(\text{S}_2\text{N}_2)\{\text{P}(\text{OR})_n\text{R}'_{3-n}\}_2]$  and  $[\text{Pt}(\text{SeSN}_2)\{\text{P}(\text{OMe})_n\text{Ph}_{3-n}\}_2]$  ( $n = 0$ –3) by straightforward and relatively low-hazard routes in liquid ammonia. In common with other S/Se–N systems the bonding in these complexes proves to be difficult to rationalise in detail. Whilst there appear to be structural trends, particularly in the selenium containing systems, these are not well modelled by the DFT calculations and further detailed work may be needed to understand the differences between experiment and calculations in these systems.

## Experimental Section

**General:** Unless otherwise stated all manipulations were performed under an oxygen-free nitrogen atmosphere, using standard Schlenk techniques and glassware. Solvents were dried and stored according to common procedures. Reagents were obtained from Aldrich and used without further purification. Solution state NMR spectra were recorded using a JEOL GSX Delta 270. Microanalyses were performed by the University of St. Andrews microanalysis service. The compound  $[\text{S}_4\text{N}_3]\text{Cl}$  was prepared by standard methods.<sup>[31]</sup> *cis*- $[\text{PtCl}_2\{\text{P}(\text{OR})_n\text{R}'_{3-n}\}_2]$  ( $\{\text{P}(\text{OR})_n\text{R}'_{3-n}\}_2 = \text{P}(\text{OPh})_3, \text{P}(\text{O}n\text{Bu})_3, \text{P}(\text{OEt})_3, \text{P}(\text{OMe})_3, \text{P}(\text{OMe})_2\text{Ph}$  or  $\text{P}(\text{OMe})\text{Ph}_2$ ) were prepared from  $[\text{PtCl}_2(\text{cyclo-octa-1,5-diene})]^{[32]}$  and two equivalents of the phosphite, phosphonite or phosphinite in dichloromethane. *cis*- $[\text{PtCl}_2(\text{PPh}_3)_2]$  was prepared via reaction of  $\text{K}_2[\text{PtCl}_4]$  in water and with  $\text{PPh}_3$  in ethanol.<sup>[33]</sup> All compounds were characterised using  $^{31}\text{P}$  NMR spectroscopy. Low solubility and sample size prevented measurement of  $^{77}\text{Se}$  NMR spectroscopy.

**CAUTION:** Reactions involving S–N compounds may generate explosive  $\text{S}_4\text{N}_4$ .  $\text{S}_4\text{N}_4$  explodes upon mechanical or heat shock. Its explosiveness increases with the purity of the substance. Kevlar gloves and visor should be used when manipulating  $\text{S}_4\text{N}_4$ . Residues of  $\text{S}_4\text{N}_4$  were disposed of by decomposition with aqueous NaOH.

**Preparation of Disulfur Dinitrido Complexes  $[\text{Pt}(\text{S}_2\text{N}_2)\{\text{P}(\text{OR})_n\text{R}'_{3-n}\}_2]$   $\{\text{PR}_3 = \text{P}(\text{OMe})_3, \text{P}(\text{OMe})_2\text{Ph}, \text{P}(\text{OMe})\text{Ph}_2, \text{P}(\text{OPh})_3, \text{P}(\text{O}n\text{Bu})_3$  or  $\text{P}(\text{OEt})_3\}$ :** In a typical reaction, liquid ammonia (30 mL) was condensed using a condenser filled with dry ice and acetone into a Schlenk tube in a dry ice/acetone bath. To this  $[\text{S}_4\text{N}_3]\text{Cl}$  (0.78 mmol) was added to produce a dark red solution. After stirring for 30 min  $[\text{PtCl}_2\{\text{P}(\text{OR})_n\text{R}'_{3-n}\}_2]$  (0.5 mmol) was added. Over the course of one hour the solution lightened to a pale orange colour. After stirring the reaction mixture at  $-78^\circ\text{C}$  for 3 h the

solution was warmed to room temp. and the ammonia was evaporated under a stream of nitrogen. The resulting pale orange residue was dried in vacuo then dissolved in dichloromethane (10 mL) and filtered through celite. The product was precipitated via slow addition of hexane. Isolated yields were 30–65%. Attempts to isolate [Pt(S<sub>2</sub>N<sub>2</sub>) {P(O*n*Bu)<sub>3</sub>}<sub>2</sub>] gave only oils. Crystals suitable for X-ray crystallography were grown by slow diffusion of hexane into a solution of the complex in dichloromethane.

**Preparation of Monoselenium Monosulfur Dinitrido Complexes [Pt(SeSN<sub>2</sub>) {P(OMe)<sub>n</sub>Ph<sub>3-n</sub>}<sub>2</sub>] (*n* = 0–3):** In a typical reaction liquid ammonia (30 mL) was condensed using a condenser filled with dry ice and acetone into a Schlenk tube in a dry ice/acetone bath. To this [S<sub>4</sub>N<sub>3</sub>]Cl (0.78 mmol) and SeCl<sub>4</sub> (3.9 mmol) were added to produce a dark red solution. Over the course of 30 min the solution became pale orange in colour. [PtCl<sub>2</sub>{P(OMe)<sub>n</sub>Ph<sub>3-n</sub>}<sub>2</sub>] (0.5 mmol) was then added. After stirring the reaction mixture at –78 °C for 3 h the solution was warmed to room temp. and the ammonia was evaporated under a stream of nitrogen. The resulting dark brown

residue was dried in vacuo then dissolved in dichloromethane (10 mL) and filtered through celite. The product was precipitated via slow addition of hexane; isolated yields were 50–75%.

Crystals suitable for X-ray crystallography were grown by slow diffusion of hexane into a solution of the complex in dichloromethane.

### Crystallography

Crystal structure data were collected for **1**, **4**, **5** and **6** at 93 K on a Rigaku MM007 confocal optics/Saturn CCD diffractometer using Mo-*K*<sub>α</sub> radiation ( $\lambda = 0.71073 \text{ \AA}$ ), for **3**, **7**, **8**, **9** and **10** at 125 K using a Rigaku SCX-Mini. All data was corrected for absorption. The structures were solved by direct methods and refined by full-matrix least-squares methods on *F*<sup>2</sup> values of all data.<sup>[34]</sup> Refinements were performed using SHELXL.<sup>[35]</sup>

CCDC-755579 (for **1**), -755580 (for **3**), -755581 (for **4**), -755582 (for **5**), -755583 (for **6**, Table 5), -766913 (for **7**), -766914 (for **8**), -766915 (for **9**), -766916 (for **10**, Table 6) contain the supplementary crystal-

Table 5. Experimental and refinement details for the X-ray structures of **1** and **3–6**.

	<b>1</b>	<b>3</b>	<b>4</b>	<b>5</b>	<b>6</b>
<i>F</i> w	[C <sub>12</sub> H <sub>18</sub> N <sub>2</sub> O <sub>6</sub> P <sub>2</sub> PtS <sub>2</sub> ]	[C <sub>36</sub> H <sub>30</sub> N <sub>2</sub> O <sub>6</sub> P <sub>2</sub> PtS <sub>2</sub> ]	[C <sub>6</sub> H <sub>18</sub> N <sub>2</sub> O <sub>6</sub> P <sub>2</sub> PtS <sub>2</sub> ]	[C <sub>16</sub> H <sub>22</sub> N <sub>2</sub> O <sub>4</sub> P <sub>2</sub> PtS <sub>2</sub> ]	[C <sub>26</sub> H <sub>26</sub> N <sub>2</sub> O <sub>2</sub> P <sub>2</sub> PtS <sub>2</sub> ]
<i>M</i>	619.54	907.77	535.37	627.51	719.64
Temperature /K	93	125	93	93	93
Crystal system	monoclinic	triclinic	monoclinic	monoclinic	orthorhombic
Space group	<i>P</i> 2 <sub>1</sub> / <i>c</i>	<i>P</i> $\bar{1}$	<i>P</i> 2(1)	<i>P</i> 2 <sub>1</sub> / <i>c</i>	<i>P</i> 2(1)2(1)2(1)
<i>a</i> / $\text{\AA}$	8.900(4)	10.8476(13)	8.299(4)	19.622(2)	10.2231(11)
<i>b</i> / $\text{\AA}$	13.719(10)	13.2659(15)	6.783(3)	13.4726(11)	14.6259(16)
<i>c</i> / $\text{\AA}$	18.519(13)	13.4783(16)	14.587(6)	18.8268	17.7113(19)
$\alpha$ /°	90	78.290(3)	90	90	90
$\beta$ /°	101.345(11)	78.106(3)	101.864	117.33(3)	90
$\gamma$ /°	90	67.963(3)	90	90	90
<i>V</i> / $\text{\AA}^3$	2217(3)	1742.3(4)	803.7(6)	4421.6(14)	2648.2(5)
<i>Z</i>	4	2	2	8	4
$\mu$ (Mo- <i>K</i> <sub>α</sub> ) /mm <sup>-1</sup>	6.689	4.288	9.207	6.704	5.604
<i>D</i> <sub>c</sub> /Mgm <sup>-3</sup>	1.856	1.730	2.212	1.885	1.805
Independent reflections ( <i>R</i> <sub>int</sub> )	4006 (0.1219)	6341 (0.1000)	2882 (0.0490)	8052 (0.0455)	4803 (0.1261)
Max. and min. transmission	0.792, 1.000	0.414, 1.000	0.740, 1.000	0.696, 1.000	0.971, 1.000
Final <i>R</i> , <i>R</i> '	0.0449, 0.1024	0.0783, 0.1748	0.0418, 0.0997	0.0353, 0.0842	0.0442, 0.1105
Largest difference peak/hole /e $\text{\AA}^{-3}$	2.591/–1.418	3.091/–2.635	2.049/–1.099	3.854/–1.439	1.394/–1.725

Table 6. Experimental and refinement details for the X-ray structures of **7–10**.

	<b>7</b>	<b>8</b>	<b>9</b>	<b>10·2H<sub>2</sub>O</b>
<i>F</i> w	[C <sub>6</sub> H <sub>18</sub> N <sub>2</sub> O <sub>6</sub> P <sub>2</sub> SSePt]	[C <sub>16</sub> H <sub>22</sub> N <sub>2</sub> O <sub>4</sub> P <sub>2</sub> SSePt]	[C <sub>26</sub> H <sub>26</sub> N <sub>2</sub> O <sub>2</sub> P <sub>2</sub> SSePt]	[C <sub>36</sub> H <sub>32</sub> N <sub>2</sub> O <sub>2</sub> P <sub>2</sub> SSePt]
<i>M</i>	582.28	674.42	766.56	894.73
Temperature /K	125	125	125	125
Crystal system	monoclinic	monoclinic	orthorhombic	triclinic
Space group	<i>P</i> 2 <sub>1</sub> / <i>c</i>	<i>P</i> 2 <sub>1</sub> / <i>n</i>	<i>P</i> 2(1)2(1)2(1)	<i>P</i> $\bar{1}$
<i>a</i> / $\text{\AA}$	15.1888(8)	9.0315(3)	10.1701(4)	11.3630(4)
<i>b</i> / $\text{\AA}$	6.8320(4)	17.8064(5)	14.7525(5)	12.1702(5)
<i>c</i> / $\text{\AA}$	16.4967(9)	13.5320(4)	18.0251(6)	16.5588(7)
$\alpha$ /°	90	90	90	93.4760(10)
$\beta$ /°	109.6816(13)	102.6458(9)	90	108.3000(10)
$\gamma$ /°	90	90	90	113.4650(10)
<i>V</i> / $\text{\AA}^3$	1611.85(15)	2123.41(11)	2704.39(17)	1948.47(13)
<i>Z</i>	4	4	4	2
$\mu$ (Mo- <i>K</i> <sub>α</sub> ) /mm <sup>-1</sup>	11.276	8.569	6.736	4.687
<i>D</i> <sub>c</sub> /Mgm <sup>-3</sup>	2.399	2.109	1.883	1.525
Independent reflections ( <i>R</i> <sub>int</sub> )	13159 (0.102)	22112 (0.063)	23268 (0.064)	16900 (0.043)
Max. and min. transmission	0.2353, 0.0930	0.4253, 0.1895	0.3451, 0.1636	0.4111, 0.2066
Final <i>R</i> , <i>R</i> '	0.0416, 0.1062	0.0326, 0.0619	0.0311, 0.0648	0.0502, 0.1545
Largest difference peak/hole /e $\text{\AA}^{-3}$	3.32/–2.19	1.51/–1.24	1.50/–0.74	2.76/–1.27

lographic data for this paper. These data can be obtained free of charge from The Cambridge Crystallographic Data Centre via [www.ccdc.cam.ac.uk/data\\_request/cif](http://www.ccdc.cam.ac.uk/data_request/cif).

### Computational Details

Geometries were fully optimised at the PBE0/ECP1 level, i.e. employing the hybrid variant of the PBE functional,<sup>[36]</sup> the Stuttgart–Dresden relativistic effective core potential (SDD ECP) along with its [6s5p3d] valence basis on Pt,<sup>[37]</sup> Binning and Curtiss' 962(d) basis on Se,<sup>[38]</sup> and 6-31G\* basis<sup>[39]</sup> elsewhere. This combination of functional and basis sets has performed very well for the description of bond lengths between third-row transition metals and their ligands.<sup>[40]</sup> For [Pt(S<sub>2</sub>N<sub>2</sub>)(PMe<sub>3</sub>)<sub>2</sub>], reoptimisation with the larger TZVP basis<sup>[41]</sup> (including the 6s4p3d1f valence basis<sup>[42]</sup> for the SDD ECP) afforded only minor changes in the Pt ligand and S–N bond lengths (typically less than 1 pm). [Pt(S<sub>2</sub>N<sub>2</sub>)(PH<sub>3</sub>)<sub>2</sub>] was reoptimised at the CCSD(T)/TZVP level, imposing C<sub>s</sub> symmetry (the minimum character of which had been confirmed by a frequency calculation at the PBE0/ECP1 level). Finally, some exploratory calculations were performed for [Pt(S<sub>2</sub>N<sub>2</sub>)(PPh<sub>3</sub>)<sub>2</sub>] at the B97-D/ECP1 level, i.e. including empirical dispersion corrections<sup>[43]</sup> that had been shown to be beneficial for the description of metal-phosphane binding energies.<sup>[44]</sup> All computations employed the Gaussian 09<sup>[45]</sup> suite of programs.

### Acknowledgments

We wish to thank Engineering and Physical Sciences Research Council (EaStCHEM) for support and access to the EaStCHEM Research Computing Facility maintained by Dr. H. Früchtl.

- [1] P. F. Kelly, J. D. Woollins, *Polyhedron* **1986**, *5*, 607–632.
- [2] P. A. Bates, M. B. Hursthouse, P. F. Kelly, J. D. Woollins, *J. Chem. Soc., Dalton Trans.* **1986**, 2367–2370.
- [3] P. S. Belton, I. P. Parkin, D. J. Williams, J. D. Woollins, *J. Chem. Soc., Chem. Commun.* **1988**, 1479–1480.
- [4] T. Chivers, F. Edelmann, U. Behrens, R. Drews, *Inorg. Chim. Acta* **1986**, *116*, 145–151.
- [5] R. Jones, P. F. Kelly, C. P. Warrens, D. J. Williams, J. D. Woollins, *J. Chem. Soc., Chem. Commun.* **1986**, 711–713.
- [6] R. Jones, P. F. Kelly, D. J. Williams, J. D. Woollins, *J. Chem. Soc., Chem. Commun.* **1985**, 1325–1326.
- [7] R. Jones, P. F. Kelly, D. J. Williams, J. D. Woollins, *Polyhedron* **1985**, *4*, 1947–1950.
- [8] R. Jones, P. F. Kelly, D. J. Williams, J. D. Woollins, *J. Chem. Soc., Dalton Trans.* **1988**, 803–807.
- [9] R. Jones, C. P. Warrens, D. J. Williams, J. D. Woollins, *J. Chem. Soc., Dalton Trans.* **1987**, 907–910.
- [10] S. M. Aucott, P. Bhattacharyya, H. L. Milton, A. M. Z. Slawin, J. D. Woollins, *New J. Chem.* **2003**, *27*, 1466–1469.
- [11] S. M. Aucott, A. M. Z. Slawin, J. D. Woollins, *Can. J. Chem.* **2002**, *80*, 1481–1487.
- [12] M. B. Hursthouse, M. Motevalli, P. F. Kelly, J. D. Woollins, *Polyhedron* **1989**, *8*, 997.
- [13] P. F. Kelly, A. M. Z. Slawin, D. J. Williams, J. D. Woollins, *Polyhedron* **1991**, *10*, 2337.
- [14] B. D. Read, A. M. Z. Slawin, J. D. Woollins, *Acta Crystallogr., Sect. E* **2007**, *63*, m751–m752.
- [15] A. A. Bhattacharyya, J. A. McLean Jr., A. G. Turner, *Inorg. Chim. Acta* **1979**, *34*, 199.
- [16] P. F. Kelly, I. P. Parkin, A. M. Z. Slawin, D. J. Williams, J. D. Woollins, *Angew. Chem. Int. Ed. Engl.* **1989**, *28*, 1047.
- [17] P. F. Kelly, A. M. Z. Slawin, D. J. Williams, J. D. Woollins, *Polyhedron* **1990**, *9*, 1567.
- [18] P. F. Kelly, J. D. Woollins, *Polyhedron* **1993**, *12*, 1129–1134.
- [19] V. C. Ginn, P. F. Kelly, J. D. Woollins, *Polyhedron* **1994**, *13*, 1501–1506.
- [20] C. A. O'Mahoney, I. P. Parkin, D. J. Williams, J. D. Woollins, *Polyhedron* **1989**, *8*, 2215–2220.
- [21] I. P. Parkin, J. D. Woollins, *J. Chem. Soc., Dalton Trans.* **1990**, 925–930.
- [22] P. F. Kelly, J. D. Woollins, *J. Chem. Soc., Dalton Trans.* **1988**, 1053–1058.
- [23] I. P. Parkin, J. D. Woollins, P. S. Belton, *J. Chem. Soc., Dalton Trans.* **1990**, 511–517.
- [24] T. Chivers, K. J. Schmidt, *J. Chem. Soc., Chem. Commun.* **1990**, 1342–1344.
- [25] M. Herberhold, W. Ehrenreich, *Angew. Chem.* **1982**, *94*, 637–638.
- [26] P. F. Kelly, I. P. Parkin, R. N. Sheppard, J. D. Woollins, *Heteroat. Chem.* **1991**, *2*, 301–3015.
- [27] F. H. Allen, A. Pidcock, C. R. Waterhouse, *J. Chem. Soc. A* **1970**, 2087–2093.
- [28] L. J. Manojlović-Muir, K. W. Muir, *Inorg. Chim. Acta* **1974**, *10*, 47–55.
- [29] Also, for a closely related system, [Pt(N=S=O)<sub>2</sub>(PMe<sub>3</sub>)<sub>2</sub>], the mean Pt–N distances at the PBE0/ECP1 level, 2.047 Å, are in excellent agreement with the X-ray data (2.049 Å for the PPh<sub>3</sub> derivative: R. Short, M. B. Hursthouse, T. G. Purcell, J. D. Woollins, *J. Chem. Soc., Chem. Commun.* **1987**, 407).
- [30] It should be noted, however, that these arguments based on a covalent σ-bonding and π-back-bonding model can be masked by more subtle electrostatic effects, see: G. Frenking, K. Wichmann, N. Fröhlich, C. Loschen, M. Lein, J. Frunzke, V. M. Rayon, *Coord. Chem. Rev.* **2003**, *238–239*, 55–82.
- [31] W. L. Jolly, M. Becke-Goering, *Inorg. Chem.* **1962**, *1*, 76–78.
- [32] J. C. Bailar, H. Itatani, *Inorg. Chem.* **1965**, *4*, 1618–1620.
- [33] F. J. Ramos-Lima, A. G. Quiroga, J. M. Pérez, M. Font-Bardía, X. Solans, C. Navarro-Ranninger, *Eur. J. Inorg. Chem.* **2003**, *8*, 1591–1598.
- [34] Rigaku, *Crystal Structure*, version 3.8 (2006), Single Crystal Structure Analysis Software, Rigaku/MSC, 9009 TX, USA 77381-5209. Rigaku, Tokyo 196-8666, Japan.
- [35] G. M. Sheldrick, *Acta Crystallogr., Sect. A* **2008**, *64*, 112–122.
- [36] a) J. P. Perdew, K. Burke, M. Ernzerhof, *Phys. Rev. Lett.* **1996**, *77*, 3865–3868; b) C. Adamo, V. Barone, *J. Chem. Phys.* **1999**, *110*, 6158–6170.
- [37] M. Dolg, U. Wedig, H. Stoll, H. Preuss, *J. Chem. Phys.* **1987**, *86*, 866–872.
- [38] R. C. Binning, L. A. Curtiss, *J. Comput. Chem.* **1990**, *11*, 1206.
- [39] a) W. J. Hehre, R. Ditchfield, J. A. Pople, *J. Chem. Phys.* **1972**, *56*, 2257–2261; b) P. C. Hariharan, J. A. Pople, *Theor. Chim. Acta* **1973**, *28*, 213–222.
- [40] M. Bühl, C. Reimann, D. A. Pantazis, T. Bredow, F. Neese, *J. Chem. Theory Comput.* **2008**, *4*, 1449–1459.
- [41] A. Schäfer, C. Huber, R. Ahlrichs, *J. Chem. Phys.* **1994**, *100*, 5829–5835.
- [42] F. Weigend, R. Ahlrichs, *Phys. Chem. Chem. Phys.* **2005**, *7*, 3297–3305.
- [43] a) S. J. Grimme, *Comput. Chem.* **2004**, *25*, 1463; b) S. J. Grimme, *Comput. Chem.* **2006**, *27*, 1787. C<sub>6</sub> parameters for Pt are not available and have been set to zero.
- [44] a) N. Sieffert, M. Bühl, *Inorg. Chem.* **2009**, *48*, 4622; b) Y. Minenkov, G. Occhipinti, V. R. Jensen, *J. Phys. Chem. A* **2009**, *113*, 11833.
- [45] M. J. Frisch, G. W. Trucks, H. B. Schlegel, G. E. Scuseria, M. A. Robb, J. R. Cheeseman, J. A. Montgomery Jr., T. Vreven, K. N. Kudin, J. C. Burant, J. M. Millam, S. S. Iyengar, J. Tomasi, V. Barone, B. Mennucci, M. Cossi, G. Scalmani, N. Rega, G. A. Petersson, H. Nakatsuji, M. Hada, M. Ehara, K. Toyota, R. Fukuda, J. Hasegawa, M. Ishida, T. Nakajima, Y. Honda, O. Kitao, H. Nakai, M. Klene, X. Li, J. E. Knox, H. P. Hratchian, J. B. Cross, V. Bakken, C. Adamo, J. Jaramillo, R. Gomperts, R. E. Stratmann, O. Yazyev, A. J. Austin, R. Cammi, C. Pomelli, J. W. Ochterski, P. Y. Ayala, K. Morok-

uma, G. A. Voth, P. Salvador, J. J. Dannenberg, V. G. Zakrzewski, S. Dapprich, A. D. Daniels, M. C. Strain, O. Farkas, D. K. Malick, A. D. Rabuck, K. Raghavachari, J. B. Foresman, J. V. Ortiz, Q. Cui, A. G. Baboul, S. Clifford, J. Cioslowski, B. B. Stefanov, G. Liu, A. Liashenko, P. Piskorz, I. Komaromi, R. L. Martin, D. J. Fox, T. Keith, M. A. Al-Laham, C. Y. Peng, A.

Nanayakkara, M. Challacombe, P. M. W. Gill, B. Johnson, W. Chen, M. W. Wong, C. Gonzalez, and J. A. Pople, *Gaussian 03*, Revision E.01, Gaussian, Inc., Wallingford CT, **2004**.

Received: March 24, 2010  
Published Online: May 31, 2010